Oncogene (2013) **32,** 4960–4969

www.nature.com/onc

**ORIGINAL ARTICLE**

# Enteropathogenic *Escherichia coli*-induced macrophage inhibitory cytokine 1 mediates cancer cell survival: an *in vitro* implication of infection-linked tumor dissemination

HJ Choi[1], J Kim[1], KH Do[1], S-H Park[1] and Y Moon[1,2]

Mucosally adherent *Escherichia coli* is frequently observed in intestinal surface of patients with colorectal cancer, but rarely in healthy control. Particularly, enteropathogenic *Escherichia coli* (EPEC) is known to be closely associated with colorectal carcinogenesis in human. In this study, one consequence of EPEC infection in human intestinal cancer cells was induction of macrophage inhibitory cytokine 1 (MIC-1), which is a multifunctional cytokine with biological activities involved in cancer cell growth, differentiation and migration. The present investigation assessed the involvement of MIC-1 protein in EPEC infection-mediated cancer cell survival. The challenge with EPEC induced cancer cell detachment via cytoskeleton rearrangement, which was positively associated with induced MIC-1 expression. Moreover, MIC-1 also mediated RhoA GTPase-linked survival of the detached cancer cells. Blocking of MIC-1 or RhoA activity increased cellular apoptosis of the detached cancer cells. In terms of signaling pathway, MIC-1 triggered transforming growth factorβ-activated kinase 1 (TAK1), which enhanced expression of RhoA GTPase. We conclude that EPEC enhances MIC-1 gene expression in the human intestinal cancer cells, which can be associated with enhanced tumor cell resistance to anchorage-dependent tumor cell death via enhanced TAK1 and RhoA GTPase.

*Oncogene* (2013) **32,** 4960–4969; doi:10.1038/onc.2012.508; published online 18 March 2013

**Keywords:** epithelial tumor cell survival; enteropathogenic *Escherichia coli*; macrophage inhibitory cytokine 1

## INTRODUCTION

Intestinal tumors, including colorectal cancer, cause nearly half a million of annual deaths, and colorectal cancer is one of the most prevalent causes of cancer-related mortality in the Western World.[1–3] For the mechanistic explanation of the intestinal epithelial carcinogenesis, environmental factor such as inflammatory responses and gut microbial influences have been recently addressed.[4,5] Experimentally, it is well documented that mucosal bacteria, including pathogens and commensals, survive in typical gut environment, which are linked with chronic inflammatory responses and intestinal carcinogenesis.[6,7] Clinical investigations suggested that mucosally adherent bacteria are more frequently identified in colon of patients with adenocarcinoma or chronic inflammatory bowel disease (IBD) than in the control, and 70% of patients with colonic adenoma and adenocarcinoma showed population dominancy of *Escherichia coli* (*E. coli*) among identified bacteria from the mucosa biopsies.[8,9] *E. coli* in the gut mucosa generally takes only $<0.1\%$ of total commensals in the healthy group.

Mucosa-associated *E. coli* groups, including enteropathogenic *E. coli* (EPEC), are human enteric pathogens that attaches to the surface of intestinal enterocytes.[10,11] Although the precise mechanism of EPEC-induced pathogenesis is presently not known, numerous studies have identified specific patterns of the pathogen on host epithelial cells. EPEC adheres to enterocytes and produces a characteristic 'attaching and effacing' lesion in the brush border membrane.[12,13] The pathogen uses a type III secretion system to deliver the effector proteins to the host epithelial cell, whose absorptive microvilli are lost (effacement).[14] After intimate interaction, enterocytes undergo cytoskeletal rearrangement such as localized polymerization of actin, which eventually leads to the formation of a pedestal-like structure below the attached bacteria.[15–19] At the level of host cell function, EPEC stimulates pro- and anti-inflammatory pathways, disrupts epithelial barrier function and alters epithelial ion and water transport, and stimulates pro- and antiapoptotic pathways.[14,20–22] In addition to the acute inflammatory pathogenesis, there have been increasing reports that mucosa-associated *E. coli* has important roles in the pathogenesis of colon cancer and chronic IBDs.[5,23] In terms of mucosal pathogen-induced carcinogenesis, murine infection model for EPEC using *Citrobacter rodentium* showed colonic hyperplasia and enhances response to chemical-induced carcinogenesis and genetic susceptibility.[23,24] Particularly, it was recently reported that EPEC suppressed DNA repair protein, which can have a potential role in human intestinal carcinogenesis.[25]

Macrophage inhibitory cytokine 1 (MIC-1, also known as prostate-derived factor, growth differentiation factor-15, placental bone morphogenetic protein, placental transforming growth factor-β and non-steroidal anti-inflammatory drug-activated protein 1)[26,27] is a divergent member of the transforming growth factor-β (TGFβ) superfamily and was first isolated from a subtracted cDNA library enriched for genes associated with macrophage activation. Although most intestinal epithelial cells

[1]Laboratory of Mucosal Exposome and Biomodulation, Department of Microbiology and Immunology and Medical Research Institute, Pusan National University School of Medicine, Yangsan, Kyungnam, Korea and [2]Research Institute for Basic Sciences and Medical Research Institute, Pusan National University, Busan, Korea. Correspondence: Professor Y Moon, Laboratory of Mucosal Exposome and Biomodulation, Department of Microbiology and Immunology and Medical Research Institute, Pusan National University School of Medicine, Room 704, Yangsan, Kyungnam 626-870, Korea.
E-mail: moon@pnu.edu
Received 10 April 2012; revised 16 August 2012; accepted 18 September 2012; published online 18 March 2013

maintain a low level of MIC-1 expression, apoptotic mucosal surface epithelial cell can induce relatively high level of MIC-1 expression.[28] Therefore, epithelial pathogenic processes, including apoptosis, inflammation and carcinogenesis, elevate the cellular levels of MIC-1 expression, implicating the protein in specific roles concerning epithelial cell behavior in stressful gut environments. MIC-1, being one of the major secreted proteins induced by p53, is thought to be important in translating p53-mediated activity associated with cell cycle arrest and apoptosis.[29] Moreover, MIC-1 has been linked to the modulation of cellular response of migrating cells in the extracellular matrix and circulation.[30,31] In colon cancer, increasing MIC-1 expression is also associated with the progression of colonic adenomas to invasive cancer and subsequent metastasis.[32] In the case of epithelial cancer, serum MIC-1 levels increase with the progression of tumor to metastasis.[32–34]

We hypothesized that EPEC could contribute to intestinal epithelial carcinogenesis by modulating tumor dissemination-associated genes, although infection-associated carcinogenesis may be a complex event of chronic inflammation and mutagenesis. As a novel modulator of EPEC infection, we investigated MIC-1-linked detachment and survival of the intestinal epithelial cancer cells. This study will address intestinal cancer cell fate by modulating cellular detachment and survival via MIC-1 in response to mucosa-associated EPEC as a potent cancer trigger in the diseased gut environment. The successful survival may enhance the chance of dissemination of epithelial cancer cells into submucosa and lymphatic circulation.

## RESULTS

### MIC-1 expression is induced by EPEC in the intestinal epithelial cancer cells

Intestinal cancer cells were evaluated via *in vitro* EPEC infection. Effects of EPEC on HCT-116 and HCT-8 human intestinal cancer cells were investigated because these cancer cells are well-recognized models for the study of intestinal epithelial carcinogenesis.[35–38] Initially, to determine whether EPEC could influence MIC-1 expression, these cell lines were treated with EPEC for defined times. As shown in HCT-116 cells in Figure 1a, MIC-1 protein was induced by EPEC exposure maximally around 4–8 h, although the cancer cells express some basal degree of MIC-1 protein. In addition, HCT-8 cells also displayed markedly enhanced MIC-1 induction in the presence of EPEC (Figure 1b). We compared EPEC with another mucosa-associated enteroaggregative *E. coli* for MIC-1 modulation. As a negative control, non-pathogenic control *E. coli* DH5$\alpha$ had no effect on the levels of MIC-1 protein. Whereas only EPEC triggered MIC-1 induction even at low density (5 bacteria per a human cell), enteroaggregative *E. coli* induced MIC-1 expression at higher density (20 bacteria per a human cell) (Figure 1c). MIC-1 induction was also shown in other cancer cells, including HT-29 and HCT-15 cells (Figure 1d). Moreover, MIC-1 was also enhanced in the colon, but not in the small intestine of mice infected with EPEC (Figure 1e). In particular, MIC-1 levels in the colonic epithelial region were highly elevated by EPEC infection (Figure 1f). Taken together, MIC-1 expression was induced by EPEC infection in human intestinal epithelial cancer cells as well as the normal colonic epithelia.

### MIC-1 expression by EPEC mediates epithelial cancer cell detachment

To address the function of EPEC-induced MIC-1 expression in cancer cells, HCT-116 colon adenocarcinoma cells were observed by phase-contrast microscopy at various times during exposure to EPEC strain E2348/69. This microscopic analysis and counting of detached cells demonstrated that EPEC induced HCT-116 cancer cell detachment, and most cancer cells were floating around 6 h after exposure (Figure 2a). Moreover, control epithelial colon cancer cells were much more susceptible to infection-induced detachment than cells with MIC-1 deficiency (Figures 2a and b), implicating MIC-1 as a critical mediator of EPEC-induced detachment of the intestinal cancer cells. Infection of cells with strains harboring mutations in *escN*, which encodes a putative ATPase for the EPEC type III secretion system had marginal effects on epithelial detachment, suggesting that epithelial detachment is dependent on type III secretion system of EPEC (Figure 2).

As EPEC is known to cause pedestal formation at the site of intimate bacterial attachment and re-organize actin-polymerization network extensively, cellular distribution and organization of F-actin were assessed to monitor changes in the cytoskeleton structure. In the control HCT-116 colon cancer cells, there was relatively dense network of unpolarized actin filaments around the cell periphery. By contrast, EPEC infection induced sequestering of actin distribution around the pedestal formation and lessened dense actin filaments around the cytoplasm (Figure 2c). However, EPEC-induced change in distribution of F-actin was rare in MIC-1-suppressed cancer cells, suggesting that MIC-1 may mediate EPEC-induced disruption of actin network in association with pedestal formation. As an extensively investigated regulator of the actin cytoskeleton in the formation of stress fibers during cancer cell migration,[39–41] RhoA GTPase was assessed along with MIC-1 protein in terms of epithelial detachment and survival from the anoikis. RhoA GTPase protein was induced by EPEC infection, which was attenuated in MIC-1-suppressed cells, indicating a positive regulation of RhoA expression by MIC-1 protein (Figure 3a). Moreover, RhoA protein was also observed in the infected cells. EPEC infection led to an upregulation of RhoA expression, which was colocalized with sequestered F-actin, the substrate of RhoA GTPase around the pedestal formation (Figure 3b). By contrast, cancer cells with interfered MIC-1 expression had less induction and sequestering of RhoA and F-actin, suggesting that MIC-1 is involved in alteration of cytoskeleton via subsequently induced RhoA GTPase in the intestinal cancer cells. RhoA was also elevated in MIC-1-expressing region in the colonic epithelia of mice infected with EPEC, but RhoA induction was almost shut down by antibiotic treatment (Figure 3c). By eradicating EPEC with antibiotic, EPEC-induced MIC1 and subsequent oncogene RhoA were downregulated (Figure 3c).

### MIC-1 and RhoA GTPase contribute to survival of detached cancer cells following EPEC infection

Migrating cancer cells maintain viability in an anchorage-independent manner to get successful metastasis and we investigated whether pathogen-induced MIC-1 can also affect survival of tumor cells. Fluorescence-activated cell sorting (FACS) analysis demonstrated that 16% of EPEC-exposed total cancer cells underwent apoptosis till 8 h (Figure 4a). However, MIC-1 interference increased death of cancer cells, which implicates the involvement of MIC-1 in survival response of the detached cancer cells. This positive association between MIC-1 induction and survival from anoikis was also confirmed using DNA fragmentation assay shown in Figure 4b. MIC-1 interference made cancer cells susceptible to apoptotic death. Moreover, the detached cancer cells were also monitored after 8 h EPEC exposure. Among the detached cancer cells by EPEC infection, more than 30% underwent apoptosis (Figure 5a). However, cells expressing shRNA MIC-1 or dominant-negative RhoA protein had more increased rate of apoptotic death after detachment. Moreover, detached cancer cells with suppressed MIC-1 expression also had less level of RhoA proteins (Figure 5b). Taken together, it can be concluded that EPEC-detached cancer cells can survive from anoikis by enhancing MIC-1 protein and subsequent RhoA GTPase.

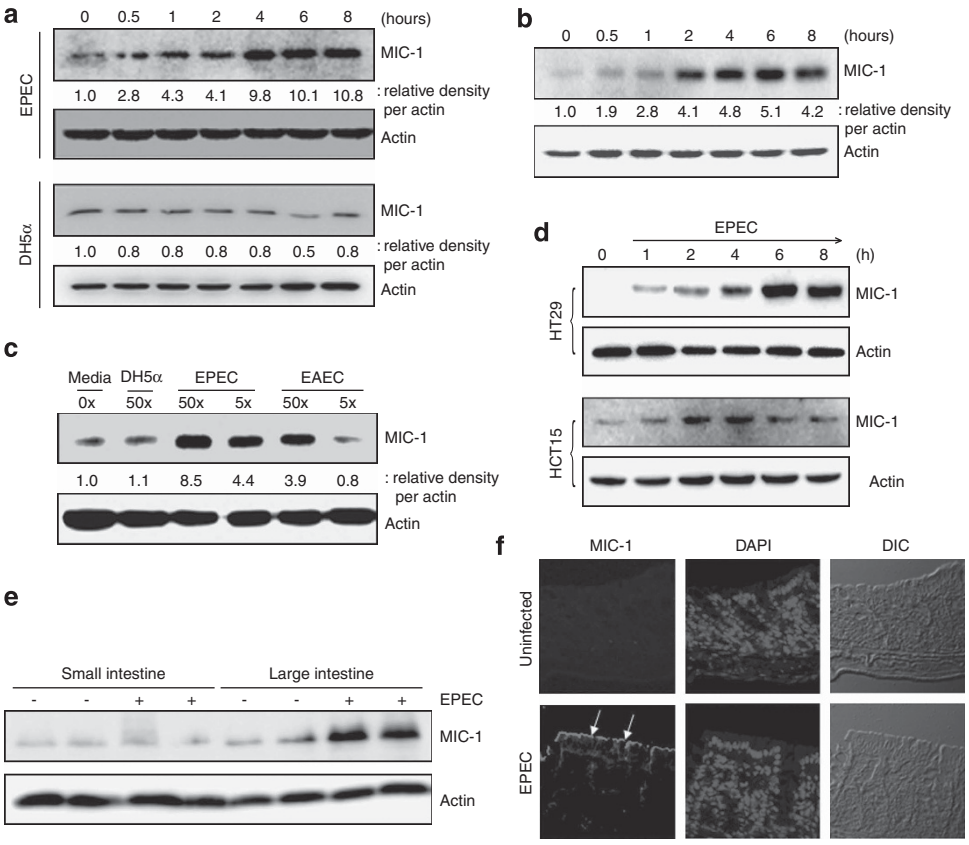


**Figure 1.** Effects of EPEC on MIC-1 expression in intestinal cancer cells. (**a**) HCT-116 human intestinal cancer cells were infected with EPEC or *E. coli* DH5α for the indicated times and the total cell lysate was examined by western blot. (**b**) HCT-8 ilocecal cancer cells were incubated with EPEC for indicated times. Total cell lysates were subjected to western blot analysis. (**c**) HCT-116 cells were infected with each fold number of or *E. coli* DH5α, EPEC and enteroaggregative *E. coli* (EAEC) for 4 h and the total epithelial cell lysate was analyzed using western blot. (**d**) HT-29 and HCT-15 human cancer cells were infected with EPEC for the indicated times and the total cell lysate was examined by western blot. (**e**, **f**) Proteins and slices from each intestinal segment of C57BL/6J mice infected with EPEC at 15th day after infection when MIC-1 expression is maximal were analyzed by western blotting or confocal microscopy, respectively. A full colour version of this figure is available at the *Oncogene* journal online.

### RhoA induction in detached cancer cells is triggered by TGFβ-activated kinase

As MIC-1 is a member of TGFβ superfamily, the signaling mediator of RhoA induction was assessed by observing TGFβ-activated kinase (TAK)-linked signaling pathway. EPEC infection activated TAK1 phosphorylation in a time-dependent manner (Figure 6a). Moreover, MIC-1 suppression reduced TAK1 phosphorylation (Figure 6b), indicating that MIC-1 mediates TAK1 activation by EPEC. Finally, TAK1 inhibition using 5Z-7-oxozeaenol, a TAK1 inhibitor, was shown to attenuate EPEC-induced RhoA expression (Figure 6c). EPEC-induced MIC-1 activated TAK1 signal, which enhanced RhoA expression in the cancer cells. The signaling patterns in the detached cells were also similar to those in the total cells infected with EPEC shown in Figure 6. Flow cytometry analysis confirmed that RhoA GTPase induction by EPEC was mediated by TAK1, which was activated by MIC-1 protein in the detached cancer cells (Figure 7).

## DISCUSSION

In this study, we provided evidences for the EPEC-associated dissemination of the intestinal cancer cells. EPEC induced MIC-1 production in human intestinal cancer cells, which was closely linked with cellular detachment and subsequent survival responses. Mechanistically, MIC-1- and TAK1-mediated RhoA protein was important in cancer cell detachment and subsequent survival from the anoikis (Figure 8). RhoA, a well-known member of the Rho family of GTPases, regulates numerous biological functions related to cancer metastasis.[39,42] Basically, enhanced RhoA activity in the cancer cells is mostly due to RhoA overexpression because mutation of RhoA has not been found in human cancers.[43,44] Accumulating evidences have shown that upregulation of *RhoA* mRNA and RhoA protein levels have been well documented in various human cancers.[45–47] This study suggests one potent mechanism of RhoA overexpression in cancer cells via MIC-1. Moreover, MIC-1-upregulated RhoA contributed to the survival and migration activity of the cancer cells in the presence of EPEC, which provides a good therapeutic target of intervention of infection-mediated cancer metastasis. However, further clinical investigation is needed to assess the correlation between MIC-1 and RhoA overexpression in the cancer patients. Although changes in MIC-1 levels are associated with a number of disease conditions, they are mostly strongly linked to cancer progression.[48,49] Increased MIC-1 expression has been documented in a variety of epithelial cancer cell lines, including breast, pancreas and colorectal cancers.[33,50,51] In colon cancer, increasing MIC-1 expression is associated with the progression of colonic adenomas to invasive cancer and subsequent metastasis.[32] As MIC-1 particularly facilitates the migration of the transformed cells, EPEC infection can facilitate dispersal of tumor cells from the original foci to the circulation and target organs, suggesting increased chances of tumor metastasis by

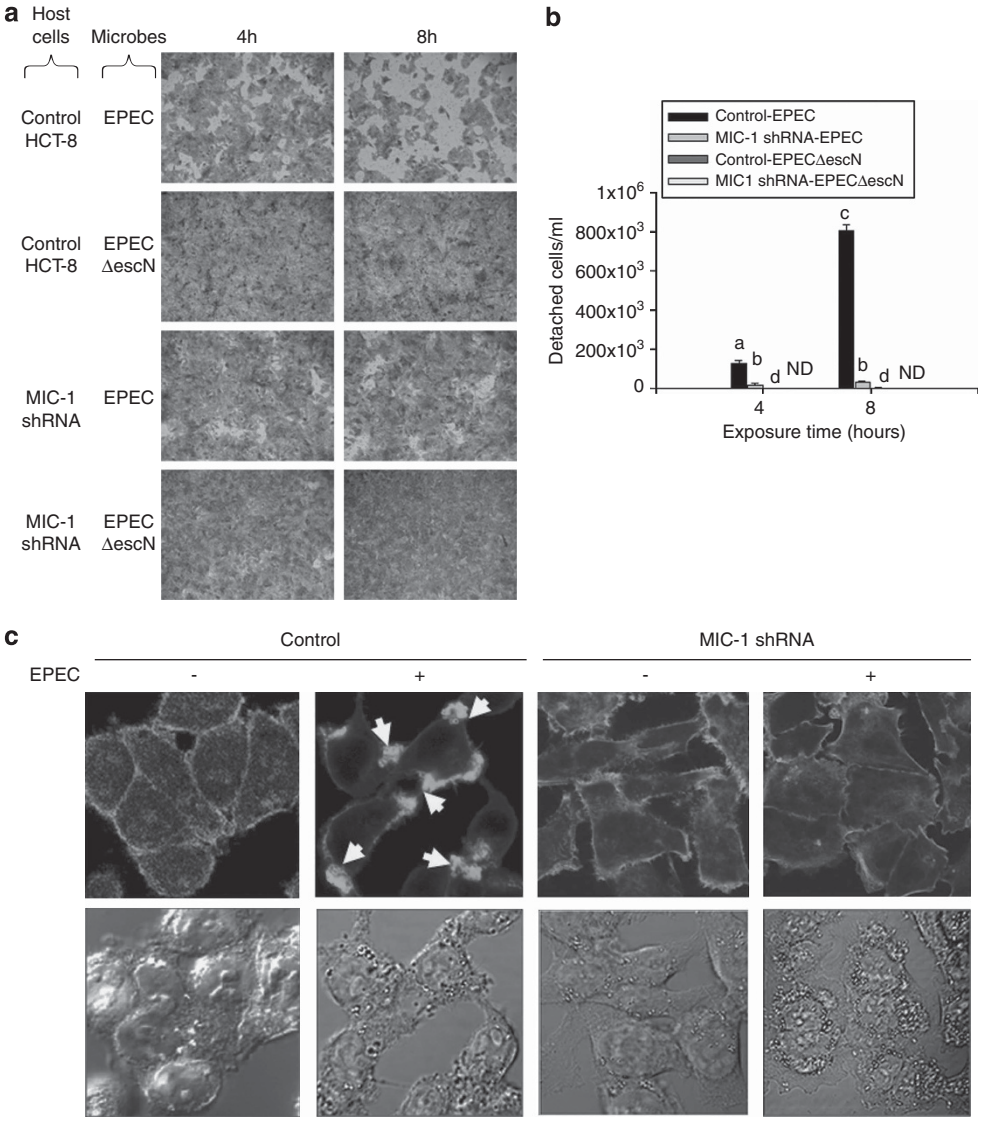


**Figure 2.** Involvement of EPEC-induced MIC-1 in detachment and morphological change. HCT-116 cells stably transfected with the empty vector (control) or MIC-1 shRNA were infected with EPEC or EPEC ΔescN for 4–8 h. After cellular fixation and staining, attached epithelial cancer cells were microscopically visualized (**a**) and detached cells were counted (**b**). (**c**) Each group of HCT-116 cells was infected with EPEC for 4 h, fixed and stained with fluorescein isothiocyanate (FITC)-conjugated phalloidin (1 μg/ml) and observed by confocal microscopy. Arrows indicate EPEC-triggered sequestering of F-actin polymers in association with pedestal formation. The different letter over each bar of the standard deviation represents significant differences between two groups by unpaired matched comparisons ($P<0.05$). ND represents 'non-detectable'. A full colour version of this figure is available at the *Oncogene* journal online.

microbial infection in cancer patients. However, parts of detached cells underwent apoptotic cell death after EPEC infection. EPEC is a non-invasive pathogen that attaches to the apical surface of the epithelial cells. Therefore, EPEC-induced MIC-1 can promote detachment of normal cells as well as the transformed cells, which can be excluded through the gut lumen. By contrast, MIC-1 also can enhance dissemination of the epithelial cancer cells from the original tumor mass. It is thus expected that some parts of detached alive cancer cells then can migrate through underlying tissue and can circulate in the body. As reported in the recent paper, mucosa-associated *E. coli*, including EPEC, promotes mutagenic insults by downregulating DNA mismatch repair protein in human colorectal adenocarcinoma cells.[25] Taken together with this study, it can be speculated that mucosal pathogen-induced carcinogenesis can be associated with MIC-1-mediated metastatic activation in tumor initiation-susceptible environment.

Along with MIC-1-mediated survival responses, transient phosphorylation of the α-subunit of translation initiation factor 2 (eIF2α) by eIF2α kinase integrates signaling in stressful conditions, reduces the rate of translation initiation (potentially suppressing the synthesis of proapoptotic proteins) and at the same time turns on genes specific to the integrated stress response, both effects contributing to cytoprotection in response to apoptotic cell death.[52,53] In the EPEC-exposed cancer cells, eIF2α-linked integrated stress response was also observed in the present model. EPEC induced integrated stress response by elevating eIF2α phosphorylation and its central effector CHOP (C/EBP Homologous Protein) in the epithelial cancer cells (Supplementary Figures 1a and b). In terms of molecular mechanism, CHOP mediated EPEC-induced MIC-1 expression. EPEC-induced CHOP enhanced MIC-1 mRNA and transcriptional activity (Supplementary Figures S1c and d) via CHOP's binding to MIC-1 promoter (Supplementary Figure S1e). In spite of the

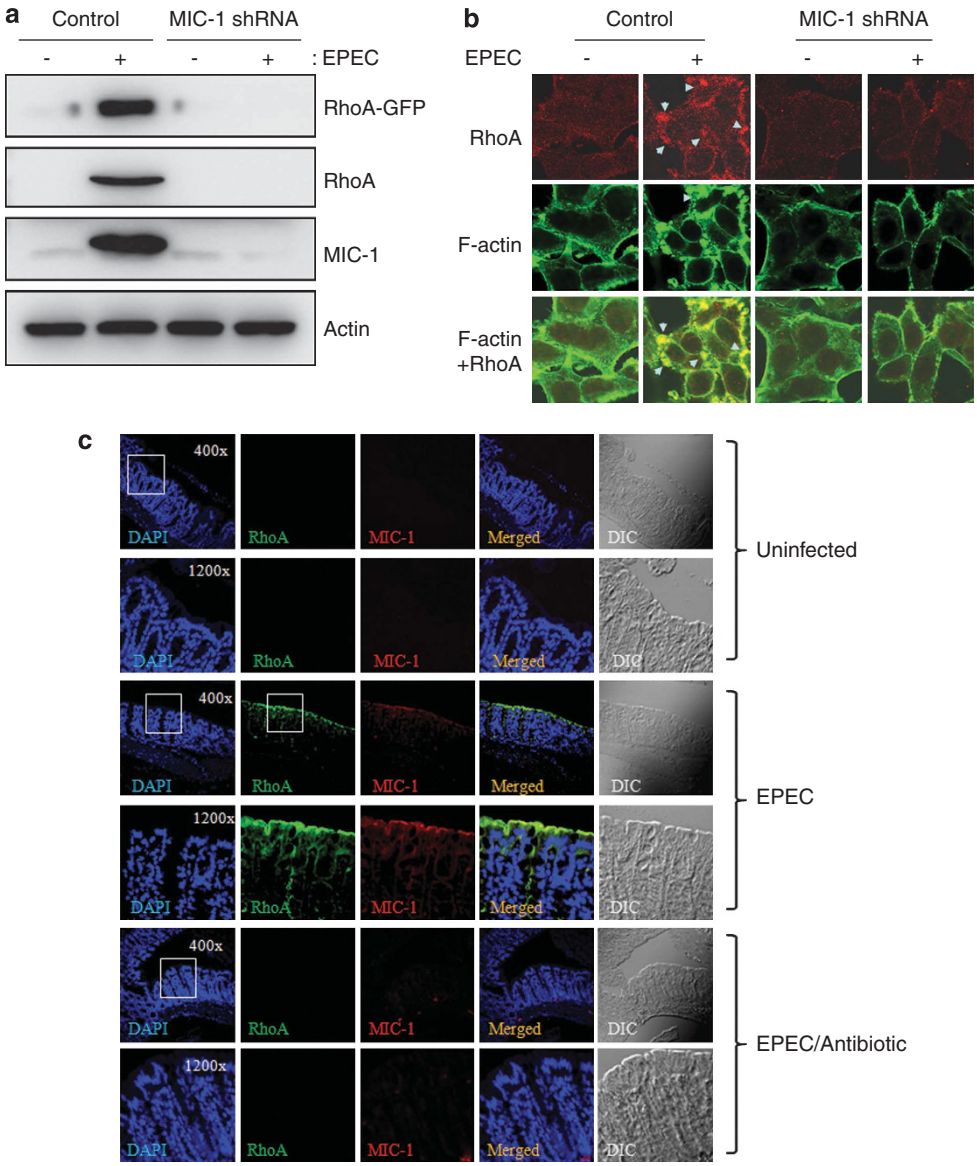


**Figure 3.** Induction of RhoA expression by MIC-1 in EPEC-infected cells. (**a**) HCT-116 cancer cells stably transfected with the empty vector (control) or MIC-1 shRNA were treated with EPEC and total cellular protein lysate was analyzed by western blot. (**b**) HCT-116 cells stably transfected with the empty vector (control) or MIC-1 shRNA were infected with EPEC. After cellular fixation and staining, attached epithelial cancer cells were microscopically visualized. (**c**) Tissue slices from colon segment of C57BL/6J mice infected with EPEC at 15th day after infection when MIC-1 expression was maximal were analyzed using confocal microscope.

antiapoptotic action of MIC-1, EPEC can also induce apoptotic cell death in normal epithelial cells. As a potent proapoptotic effector, EspF has been demonstrated to induce epithelial apoptosis by attenuating antiapoptotic function of mammalian ribosomal Abcf2.[54,55] Abcf2 belongs to ABC transporter superfamily and interact with eIF2$\alpha$, which has a key role in the control of translational arrest. Therefore, one possible speculation can be that bacterial EspF modulates epithelial integrated stress response via Abcf2-associated pathways. In response to the proapoptotic action, cells develop defensive responses via MIC-1-linked machinery.

Other several MIC-linked factors have been suggested for their possible involvement in mucosal microenvironment. MIC-1 provides pathogenic environment favorable for the cancer growth and metastasis of epithelial cells. MIC-1 and its target oncogenes, including RhoA, enhanced cellular survival after epithelial detachment in the tumor microenvironment. RhoA was elevated in MIC-1-expressing region in the colonic epithelial cells, but it was almost shut down in antibiotic-treated mouse since MIC-1 was not induced. We reported that MIC-1 modulates gene expression of plasminogen activator urokine (PLAU) and plasminogen activator receptor (PAR).[35] Moreover, RhoE and catenin $\delta$1 are target molecules of MIC-1 during tumor cell metastasis.[30] All the four known target molecules (PLAU, PAR, RhoE and catenin $\delta$1) were also enhanced by EPEC in the murine infection model, but were decreased by antibiotic treatment (Supplementary Figure S2a). As MIC-1 have key roles in cancer cell survival, blocking of its target molecules, including PLAU and PAR activity, increased cellular survival after cell detachment (Supplementary Figure S2b). In addition to PLAU and PAR, catenin $\delta$1 and RhoE are both associated with intercellular adhesion receptors, such as cadherin at the intercellular junction, which are essential for the establishment of the cell shape, maintenance of the differentiated phenotype and adherence junctions between cells.[30,56]

The whole additional studies support the opinion that MIC-1 can be a potent convergence point of coordinating cellular survival and resistance to infection-induced apoptosis.

As MIC-1 can be induced by EPEC in the normal epithelial tissue, its role in the microbial infection should also be assessed. Infection-mediated detachment of normal intestinal epithelial cells does not always prelude negative effects in the host. MIC-1 can aid host defense by shedding of luminal EPEC-attached gut epithelia, which may reduce the chance of the mucosal pathogenicity by the non-invasive pathogen. In contrast, pathogen-disrupted gut barrier can be more susceptible to the next microbial translocation such as pathogens and commensal microbes, which is a critical etiological factor of IBD.[57,58] Mucosa-associated *E. coli* strains with mannose-resistant adhesion have a crucial role in the pathogenesis of IBD.[9,59] Moreover, compared with control group with no history of IBD, patients with ulcerative colitis shows more enhanced production of human α-defensins 5 and 6, β-defensins 1 and 2 and lysozyme, which are involved in the first line of defense against pathogenic *E. coli*.[60] It can be thus suggested that mucosa-associated *E. coli* may contribute to the onset or chronicity of IBD via MIC-1 pathway.

Conclusively, challenge with EPEC induced cancer cell detachment and survival, which were associated with MIC-1 induction, implicating tumor dissemination into submucosa and lymphatic circulation *in vivo*. Detached cells can suffer from apoptotic death, but many of them survive and reattach by virtue of MIC-1-linked factor, including TAK1 and RhoA GTPase protein. Infection-associated carcinogenesis may be a complex event of chronic inflammation and mutagenesis. It is thus warranted in the future study to investigate therapeutic strategies to suppress intestinal epithelial carcinogenesis by mitigating MIC-1-linked pathogenicity of mucosa-associated *E. coli*.

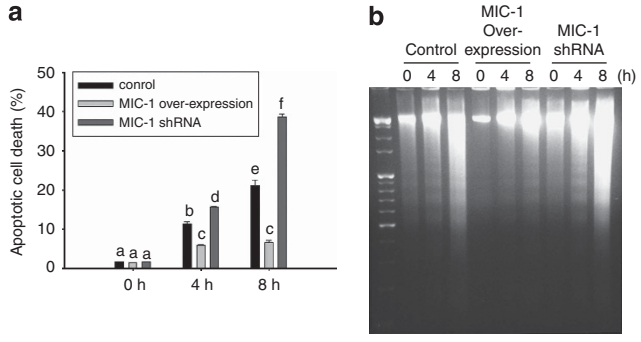


**Figure 4.** Role of MIC-1 in survival of detached cancer cells in response to EPEC infection. (**a**) HCT-116 cancer cells stably transfected with the empty vector (control), MIC-1 cDNA (MIC-1 overexpression) plasmid or MIC-1 shRNA-expressing vector were infected with EPEC for 4 or 8 h and stained with propidium iodide (PI) to analyze cell death by FACS. Total cells were analyzed separately. The different letter over each bar of the standard deviation represents significant differences between two groups by unpaired matched comparisons ($P<0.05$). (**b**) HCT-116 cancer cells stably transfected with the empty vector (control) MIC-1 cDNA (MIC-1 overexpression) plasmid or MIC-1 shRNA-expressing vector were infected with EPEC for 4 or 8 h and the fragmented DNA was analyzed by the protocols indicated in the section of 'Materials and methods'.

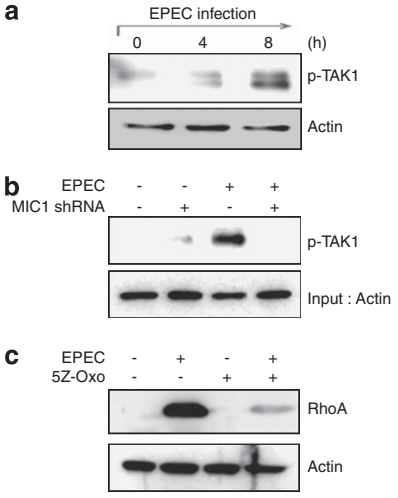


**Figure 6.** Signaling cascade from MIC-1 to RhoA induction in EPEC-infected total cancer cells. (**a**) HCT-116 cells were infected with EPEC for the indicate time and the total cell lysate was examined by western blot. (**b**) HCT-116 cancer cells stably transfected with the empty vector (control) or MIC-1 shRNA were infected with EPEC for 8 h and the total cell lysate was examined by western blot. (**c**) HCT-116 cells were pretreated with vehicle (dimethylsulfoxide (DMSO)) or 100 nM 5Z-7-oxozeaenol for 2 h and then treated with EPEC for 8 h. The total cell lysate was examined by western blot.

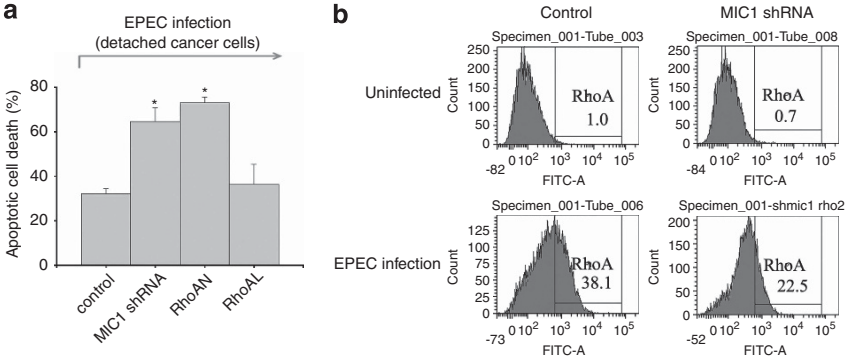


**Figure 5.** Roles of RhoA and MIC-1 in survival of the EPEC-detached cells. (**a**) HCT-116 cancer cells were stably transfected with the empty vector (control), MIC-1 shRNA, dominant-negative RhoA plasmid (RhoAN; T19N substitution), activated form of Rho A expression plasmid (RhoAL; Q63L substitution). After infection with EPEC for 8 h, the detached cells were stained with propidium iodide (PI) to analyze cell death by FACS. Groups with asterisk are significantly different ($P<0.05$) from the control infected cell group. (**b**) HCT-116 cancer cells stably transfected with the empty vector (control) or MIC-1 shRNA were infected with EPEC. The detached cells were stained for RhoA expression and microscopically visualized. The italic numbers in the each box indicate the relative % of the RhoA expression over the control uninfected group.

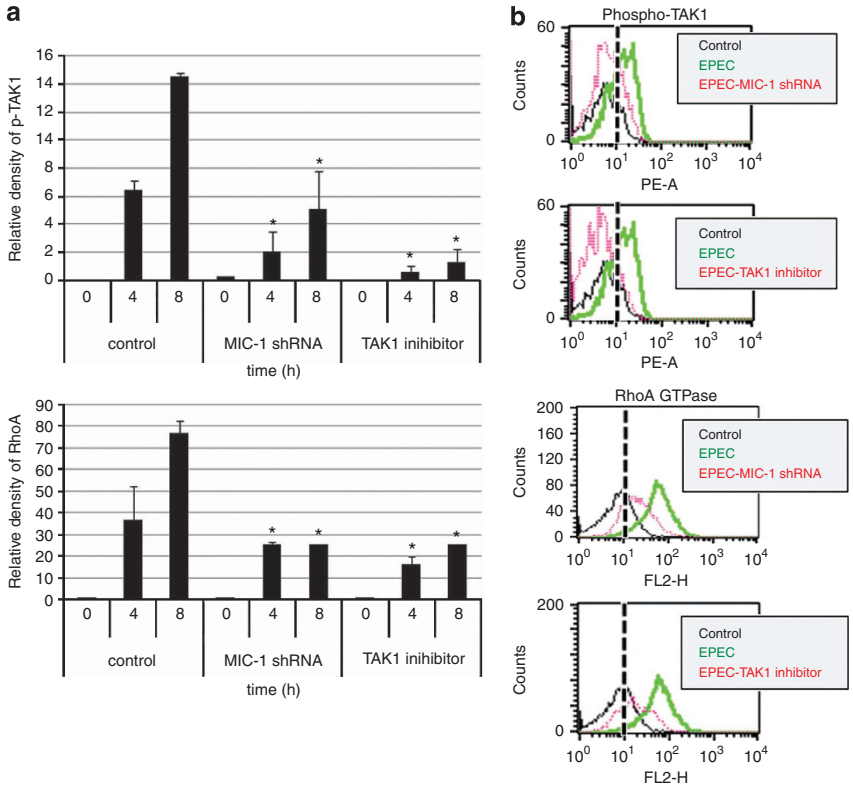


**Figure 7.** Signaling cascade from MIC-1 to RhoA induction in EPEC-infected detached cancer cells. HCT-116 cancer cells stably transfected with the empty vector (control) or MIC-1 shRNA were pretreated with vehicle (dimethylsulfoxide (DMSO)) or 100 nM 5Z-7-oxozeaenol for 2 h, and then infected with EPEC for 8 h. The detached cells were stained using anti-phospho-TAK1 antibody (**a**) or anti-RhoA GTPase antibody and quantified for relative staining. Figures in each right box are representative data of the TAK1 (**a**) or RhoA protein (**b**) expression in the detached cells analyzed by FACS flow cytometry. The symbol '*' indicates the significant difference from the control group at each time point following infection ($P < 0.05$).

## MATERIALS AND METHODS

### Cell culture conditions and reagents

The HCT-116 and HCT-8 human intestinal epithelial cancer cell line was purchased from the American Type Culture Collection (Rockville, MD, USA). Cells were maintained in RPMI medium (Invitrogen, Carlsbad, CA, USA) supplemented with 10% (v/v) heat-inactivated fetal bovine serum (Sigma-Aldrich, St Louis, MO, USA), 50 U/ml penicillin (Sigma-Aldrich) and 50 μg/ml streptomycin (Sigma-Aldrich) in a 5% $CO_2$ humidified incubator at 37 °C. Cell number and viability were assessed using a standard assay of the exclusion of Trypan blue dye (Sigma-Aldrich). However, during the infection step, cells were incubated in antibiotic-free media after several washing in antibiotics-free RPMI media.

### Bacterial strains and infection

Wild-type EPEC used for all experiments was the *E. coli* O127 strain E2348/69. EPEC mutant in type III secretion system-related ATPase gene *escN* (EPEC ΔescN) was kindly provided by Dr Ilan Rosenshine (The Hebrew University, Jerusalem, Israel) and Dr James Kaper (University of Maryland, Baltimore, MD, USA). Briefly, bacteria were shaken in LB broth (Duchefa Biochemie, Haarlem, The Netherlands) at 37 °C overnight. Bacteria were further subcultured in antibiotic- and serum-free RPMI-1640 with 1% mannose at 37 °C to get absorbance optic density (OD) of 0.5–0.6 at 600 nm. EPEC were then added to the apical surface of HCT-116 cell culture at a ratio of 50:1 (bacteria to cell). Bacteria were grown to stationary phase in LB broth containing the appropriate antibiotics. For mouse EPEC infection, 6- to 8-week-old C57BL/6J mice were purchased from Jackson Laboratories (Bar Harbor, MN, USA) and allowed to acclimate for 7 days. All mice were individually housed in ventilated cages with free access to food and water. EPEC were grown to stationary phase in LB broth. Aliquots of the broth culture (1 ml) were centrifuged and the bacterial pellet was suspended in 1.25 ml phosphate-buffered saline (PBS). A suspension containing approximately $2 \times 10^8$ E2348/69 cells in 200 μl of PBS were introduced into the animals by gavage with a curved needle 4 cm in length with a steel ball at the tip. Control animals received 200 μl sterile PBS and the antibiotic treatments were performed by adding 2 mg/ml streptomycin in the drinking water for 7 days after EPEC infection. Over the course of infection, the mice were observed daily to assess activity levels and water intake, and body weight was measured. At various times following infection (2, 5, 8, 10 and 13 days), the animals were killed and intestinal tissues were processed for further analysis.

### Western immunoblot analysis

Cells were washed with ice-cold phosphate buffer, lysed in boiling lysis buffer consisting of 1% (w/v) sodium dodecyl sulfate (SDS), 1.0 mM sodium orthovanadate and 10 mM Tris (pH 7.4) and sonicated for 5 s. Lysate containing proteins were quantified using a BCA protein assay kit (Pierce, Rockford, IL, USA). In all, 50 micrograms of protein was separated by 10% SDS–polyacrylamide gel electrophoresis (SDS–PAGE) using a mini gel apparatus (Bio-Rad, Hercules, CA, USA). Proteins were transferred onto a polyvinylidene fluoride membrane (Amersham Pharmacia Biotech, Piscataway, NJ, USA) and each membrane was blocked with 5% skim milk in Tris-buffered saline plus Tween 0.05% (TBST). Protein bands were probed with primary antibody followed by labeling with horseradish peroxidase-conjugated anti-mouse, anti-rabbit or anti-goat secondary antibody. The antibodies used were: anti-MIC1, anti-phospho-ERK, anti-PARP (Santa Cruz Biotechnology, Santa Cruz, CA, USA) and anti-phospho-AKT (Cell Signaling Technology, Beverly, MA, USA). Bands were visualized by enhanced chemiluminescence (Amersham Pharmacia Biotech, Piscataway, NJ, USA) according to the manufacturer's instruction.

### Conventional and real-time reverse transcription–polymerase chain reaction

Total RNA was extracted from cells using Qiazol (Qiagen, Valencia, CA, USA) and the RNA concentration was determined from the absorbance at 260 nm. First-strand DNA was reverse transcribed from 1 μg of total RNA in a final volume of 20 μl. The DNA was added to a 20 μl polymerase chain

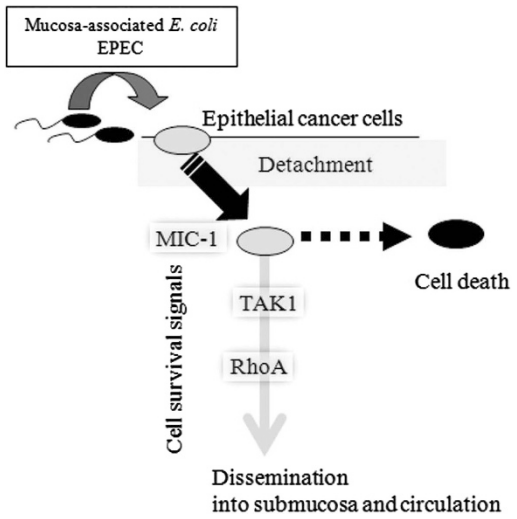


**Figure 8.** Putative mechanism of EPEC-infected cancer cell survival. The schematic signaling patterns illustrate that EPEC induces MIC-1 expression, which triggers the detachment of intestinal cancer cells. Detached cells can suffer from apoptotic death, but many of them survive and disseminate by virtue of MIC-1-linked factors, including TAK1 and RhoA GTPase protein. A full colour version of this figure is available at the *Oncogene* journal online.

reaction (PCR) reaction mixture with each set of gene-specific primers: The 5′ forward- and 3′ reverse-complement PCR primers for amplification of each gene were as follows: human MIC-1 (F: 5′-ACGCTACGAGGACCTGCTAA-3′; R: 5′-AGATTCTGCCAGCAGTTGGT-3′); mouse MIC-1 (F: 5′-GACATCACTAGGCCC CTGAA-3′; R: 5′-GATACAGGTGGGGACACTCG-3′); mouse PLAU (F: 5′-AGTGTGGCCAGAAGGCTCTA-3′; R: 5-CCCGTGCTGGTACGTA TCTT-3′); mouse PAR (F: 5′-GCCGCTATCCTACAGAGCAC-3′; R: 5′-GTAGCCACCAGGCACTGATT-3′); mouse RhoE (F: 5′-TCTTCGCTTTGTCCTTTCGT-3′; R: 5′-CCTGTGGGACACTTCAGGTT-3′); mouse catenin Δ1 (F: 5′-CCAGACTTT GGGTCGTGATT-3′; R: 5′-GCCCATACTACGCTGGTCAT-3′) and human/mouse GAPDH (F: 5′-TCAACGGATTTGGTCGTATT-3′; R: 5′-CTGTGGTCATGAGTC CTTCC-3′). The thermal cycling conditions used consisted of initial denaturation at 94 °C for 4 min, followed by 28 cycles of 94 °C for 30 s, 58 °C for 30 s and 73 °C for 45 s and a final extension for 10 min at 72 °C. The final PCR products were electrophoresed on a 1% agarose gel and photographed under ultraviolet illumination. In the real-time PCR, FAM (6-carboxyl-fluorescein) was used as a fluorescent reporter dye and conjugated to the 5′ ends of the probes to detect amplified cDNA in the iCycler Thermal Cycler (Bio-Rad) using the following parameters: denaturation at 94 °C for 2 min and 40 cycles of reactions of denaturation at 98 °C for 10 s, annealing at 59 °C for 30 s and elongation at 72 °C for 45 s. Each sample was tested in triplicate to ensure statistical significance. Gene expression was quantified using the comparative $C_t$ method. The $C_t$ value is defined as the point where a statistically significant increase in the fluorescence has occurred. The number of PCR cycles ($C_t$) required for the FAM intensities to exceed a threshold just above background was calculated for the test and reference reactions. In all experiments, GAPDH was used as the endogenous control. Results were analyzed as a relative quantity based on vehicle-treated samples.

## Stable transfection

MIC-1 shRNA expression vector was kindly provided by Dr Jong-Sik Kim (Andong National University, Gyeongsangbuk Korea) and Dr Seong-Joon Baek (The University of Tennessee, Knoxville, TN, USA). The activated form of Rho A expression plasmid (Q63L substitution) and dominant-negative RhoA plasmid (T19N substitution) was provided from Upstate Biotech (Lake Placid, NY, USA). Expression plasmid for dominant-negative CHOP was kindly provided by Dr Tomomi Gotoh of Kumamoto University (Kumamoto, Japan).[61] Cells were transfected using Trans-LT1 transfection reagent (Mirus, Madison, WI, USA) according to the manufacturer's protocol. MIC-1 shRNA expression vector was co-transfected with pcDNA3.1-neo. Following transfection, cells underwent 2 weeks of selection with 400 μg/ml G418 (Life Technologies, Korea LLC, Seoul, Korea). Single colonies were expanded and maintained in medium with 200 μg/ml G418. All transfection efficiencies were maintained at around 50–60%, which was confirmed with pMX-enhanced GFP vector.

## Rho activation assay

GST-Rhotekin RBD was produced in *E. coli* (DH5 strain). Bacterial cultures were grown to $A_{600} = 0.6$ and then induced with 5 mM isopropyl-β-D-thiogalactopyranoside for 4 h at 4 °C. The bacteria were harvested in lysis buffer (50 mM Tris, pH 7.4, 150 mM NaCl, 5 mM $MgCl_2$, 1% Triton X-100) containing protease inhibitors and were lysed by sonication (8 × 15 s on ice). After centrifugation (12 000 *g* for 30 min at 4 °C), the GST-Rhotekin-RBD was collected from the clarified supernatant by rocking at 4 °C for 45 min with glutathione-agarose (Santa Cruz Biotechnology). The bead was washed three times with assay buffer, resuspended in fresh buffer and aliquots snap frozen in liquid $N_2$ for future use. Cultured cells were rinsed with Tris-buffered saline and lysed in buffer (250 mM Tris-HCl (pH 8.7), 750 mM NaCl, 50 mM $MgCl_2$, 5 mM EDTA, 5% Triton X-100) containing protease inhibitors. The lysates were clarified by brief centrifugation and then incubated with the agarose bead-bound GST-Rhotekin-RBD for 45 min at 4 °C. The beads and precipitated proteins were washed four times in cold lysis buffer and then the proteins were eluted by boiling in Laemmli buffer and separated by SDS–PAGE. Proteins were immunoblotted with Rho-specific antibodies (Santa Cruz Biotechnology), followed by detection with horseradish peroxidase-conjugated secondary antibodies. The precipitated Rho was normalized to the Rho present in whole cell lysate.

## Luciferase assay

Cells were washed with cold PBS, lysed with passive lysis buffer (Promega, Korea, LTD. Seoul, Korea) and then centrifuged at 12 000 *g* for 4 min. The supernatant was collected isolated and stored at − 80 °C until assessment of luciferase activity. Luciferase activity was measured with a dual-mode luminometer (Model TD-20/20; Turner Designs, Sunnyvale, CA, USA) after briefly mixing the supernatant (10 μl) with 50 μl firefly luciferase assay substrate solution, followed with 50 μl stop solution (Promega). Luciferase activity was normalized by dividing firefly luciferase activity by Renilla luciferase activity.

## Confocal microscopy

After treatment with EPEC or control bacteria, cells were fixed with 4% formaldehyde diluted in PBS (USB, Cleveland, OH, USA). Fixed cells were permeabilized with 0.1% NP-40 in PBS for 10 min. After 1 h blocking with 3% bovine serum albumin in PBS, cells were stained with 100 ng/ml fluorescein isothiocyanate (Sigma-Aldrich) in PBS for 30 min. Fluorescent microscope images were obtained using a Fluoview 1000 confocal laser scanning microscope (Olympus, Tokyo, Japan) using a single line (520 nm). Images were acquired and processed with FV10-ASW version 1.7 software (Olympus).

## Chromatin immunoprecipitation assay

Cells were crosslinked for 10 min in 1% formaldehyde. The reaction was stopped by the addition of glycine to 125 mM, and cells were washed twice with 1 × PBS. Chromatin was fragmented by sonication for 10 s to a size of 1000–2000 bp in lysis buffer (1% (w/v) SDS, 10 mM EDTA, pH 8.0, 50 mM Tris-HCl, pH 8.0), protease inhibitor mixture) using Vibra-Cell (Sonics and Materials, Newtown, CT, USA). The soluble chromatin was immunoprecipitated with 2 μg of mouse monoclonal anti-CHOP antibody in a mixture of nine parts dilution buffer (1% Triton X-100, 150 mM NaCl, 2 mM EDTA, pH 8.0, 20 mM Tris (pH 8.0) and protease inhibitor mixture) and one part lysis buffer. After rotating overnight at 4 °C, protein G-Sepharose 4 fast flow (GE Healthcare, Wauwatosa, WI, USA) was added in 100 μl of a 9:1 mixture of dilution buffer and lysis buffer containing 100 μg/ml bovine serum albumin) and 500 μg/ml salmon sperm DNA (Invitrogen) per sample. After centrifugation of the protein G-Sepharose mixture, each sample was washed twice in dilution buffer, and finally the chromatin was resuspended in the 9:1 dilution buffer/lysis buffer solution and incubated at 37 °C with proteinase K and RNase A (500 μg/ml for each sample). Chromatin was purified using a MEGAquick-spinTM kit (Intron, SungNam, South Korea).

### FACS analysis

HCT-116 cells ($5 \times 10^5$) were plated, incubated and then treated with EPEC. After treatment, the cells were harvested, washed with PBS, fixed by the slow addition of cold 70% ethanol to a total of 1 ml and stored at 4 °C overnight. The fixed cells were pelleted, washed once with PBS and stained with propidium iodide and RNase in PBS for 20 min. Cells were examined by flow cytometry using a FACSort apparatus (BD Biosciences, Franklin Lakes, NJ, USA) equipped with CellQuest software (BD Biosciences) by gating on an area-versus-width dot plot to exclude cell debris and cell aggregates. Apoptosis was measured by the level of subdiploid DNA contained in cells after treatment with EPEC2348/69 using CellQuest software.

### Statistical analyses

Data were analyzed using SigmaStat for Windows (Jandel Scientific, San Rafael, CA, USA). For comparison of two groups of data, Student's *t*-test was performed. For comparison of multiple groups, data were subjected to analysis of variance and pairwise comparisons made by the Student–Newman–Keuls method.

## CONFLICT OF INTEREST

The authors declare no conflict of interest.

## ACKNOWLEDGEMENTS

This work was supported by the Basic Science Research Program through the National Research Foundation of Korea, funded by Ministry of Education, Science and Technology Grant 2012R1A1A2005837.

## REFERENCES

1 Thompson PA, Gerner EW. Current concepts in colorectal cancer prevention. *Expert Rev Gastroenterol Hepatol* 2009; **3**: 369–382.
2 Potter JD, Slattery ML, Bostick RM, Gapstur SM. Colon cancer: a review of the epidemiology. *Epidemiol Rev* 1993; **15**: 499–545.
3 Lieberman D. Colon cancer screening and surveillance controversies. *Curr Opin Gastroenterol* 2009; **25**: 422–427.
4 Triantafillidis JK, Nasioulas G, Kosmidis PA. Colorectal cancer and inflammatory bowel disease: epidemiology, risk factors, mechanisms of carcinogenesis and prevention strategies. *Anticancer Res* 2009; **29**: 2727–2737.
5 Mager DL. Bacteria and cancer: cause, coincidence or cure? A review. *J Transl Med* 2006; **4**: 14.
6 Rogers AB, Houghton J. Helicobacter-based mouse models of digestive system carcinogenesis. *Methods Mol Biol* 2009; **511**: 267–295.
7 Rogers AB, Fox JG. Inflammation and cancer. I. Rodent models of infectious gastrointestinal and liver cancer. *Am J Physiol Gastrointest Liver Physiol* 2004; **286**: G361–G366.
8 Swidsinski A, Khilkin M, Kerjaschki D, Schreiber S, Ortner M, Weber J *et al.* Association between intraepithelial *Escherichia coli* and colorectal cancer. *Gastroenterology* 1998; **115**: 281–286.
9 Martin HM, Campbell BJ, Hart CA, Mpofu C, Nayar M, Singh R *et al.* Enhanced *Escherichia coli* adherence and invasion in Crohn's disease and colon cancer. *Gastroenterology* 2004; **127**: 80–93.
10 Stypulkowska-Misiurewicz H, Truchanowicz-Jarmolowicz Z, Noworyta J. Role of pathogenic strains of *Escherichia coli* (EPEC and ETEC) in the etiology of infantile diarrhea. *Przegl Epidemiol* 1984; **38**: 19–27.
11 Oliva CA, Scaletsky I, de Morais MB, Fagundes Neto U. Severe acute diarrhea associated to classic enteropathogenic *Escherichia coli* (EPEC): clinical features and fecal losses in hospitalized infants. *Rev Assoc Med Bras* 1997; **43**: 283–289.
12 Rothbaum R, McAdams AJ, Giannella R, Partin JC. A clinicopathologic study of enterocyte-adherent *Escherichia coli*: a cause of protracted diarrhea in infants. *Gastroenterology* 1982; **83**: 441–454.
13 Ulshen MH, Rollo JL. Pathogenesis of escherichia coli gastroenteritis in man—another mechanism. *N Engl J Med* 1980; **302**: 99–101.
14 Dean P, Maresca M, Schuller S, Phillips AD, Kenny B. Potent diarrheagenic mechanism mediated by the cooperative action of three enteropathogenic *Escherichia coli*-injected effector proteins. *Proc Natl Acad Sci USA* 2006; **103**: 1876–1881.
15 Batchelor M, Guignot J, Patel A, Cummings N, Cleary J, Knutton S *et al.* Involvement of the intermediate filament protein cytokeratin-18 in actin pedestal formation during EPEC infection. *EMBO Rep* 2004; **5**: 104–110.
16 Campellone KG, Leong JM. Tails of two Tirs: actin pedestal formation by enteropathogenic *E. coli* and enterohemorrhagic *E. coli* O157:H7. *Curr Opin Microbiol* 2003; **6**: 82–90.
17 Matsuzawa T, Kuwae A, Yoshida S, Sasakawa C, Abe A. Enteropathogenic *Escherichia coli* activates the RhoA signaling pathway via the stimulation of GEF-H1. *EMBO J* 2004; **23**: 3570–3582.
18 Tomson FL, Viswanathan VK, Kanack KJ, Kanteti RP, Straub KV, Menet M *et al.* Enteropathogenic *Escherichia coli* EspG disrupts microtubules and in conjunction with Orf3 enhances perturbation of the tight junction barrier. *Mol Microbiol* 2005; **56**: 447–464.
19 Viswanathan VK, Lukic S, Koutsouris A, Miao R, Muza MM, Hecht G. Cytokeratin 18 interacts with the enteropathogenic *Escherichia coli* secreted protein F (EspF) and is redistributed after infection. *Cell Microbiol* 2004; **6**: 987–997.
20 Hecht G. Microbes and microbial toxins: paradigms for microbial–mucosal interactions. VII. Enteropathogenic *Escherichia coli*: physiological alterations from an extracellular position. *Am J Physiol Gastrointest Liver Physiol* 2001; **281**: G1–G7.
21 Crane JK, Majumdar S, Pickhardt III DF. Host cell death due to enteropathogenic *Escherichia coli* has features of apoptosis. *Infect Immun* 1999; **67**: 2575–2584.
22 Borthakur A, Gill RK, Hodges K, Ramaswamy K, Hecht G, Dudeja PK. Enteropathogenic *Escherichia coli* inhibits butyrate uptake in Caco-2 cells by altering the apical membrane MCT1 level. *Am J Physiol Gastrointest Liver Physiol* 2006; **290**: G30–G35.
23 Newman JV, Kosaka T, Sheppard BJ, Fox JG, Schauer DB. Bacterial infection promotes colon tumorigenesis in $Apc_{(Min/+)}$ mice. *J Infect Dis* 2001; **184**: 227–230.
24 Barthold SW, Jonas AM. Morphogenesis of early 1, 2-dimethylhydrazine-induced lesions and latent period reduction of colon carcinogenesis in mice by a variant of *Citrobacter freundii*. *Cancer Res* 1977; **37**: 4352–4360.
25 Maddocks OD, Short AJ, Donnenberg MS, Bader S, Harrison DJ. Attaching and effacing *Escherichia coli* downregulate DNA mismatch repair protein *in vitro* and are associated with colorectal adenocarcinomas in humans. *PLoS One* 2009; **4**: e5517.
26 Fairlie WD, Moore AG, Bauskin AR, Russell PK, Zhang HP, Breit SN. MIC-1 is a novel TGF-beta superfamily cytokine associated with macrophage activation. *J Leukoc Biol* 1999; **65**: 2–5.
27 Bootcov MR, Bauskin AR, Valenzuela SM, Moore AG, Bansal M, He XY *et al.* MIC-1, a novel macrophage inhibitory cytokine, is a divergent member of the TGF-beta superfamily. *Proc Natl Acad Sci USA* 1997; **94**: 11514–11519.
28 Kim KS, Baek SJ, Flake GP, Loftin CD, Calvo BF, Eling TE. Expression and regulation of nonsteroidal anti-inflammatory drug-activated gene (NAG-1) in human and mouse tissue. *Gastroenterology* 2002; **122**: 1388–1398.
29 Agarwal MK, Hastak K, Jackson MW, Breit SN, Stark GR, Agarwal ML. Macrophage inhibitory cytokine 1 mediates a p53-dependent protective arrest in S phase in response to starvation for DNA precursors. *Proc Natl Acad Sci USA* 2006; **103**: 16278–16283.
30 Liu T, Bauskin AR, Zaunders J, Brown DA, Pankhurst S, Russell PJ *et al.* Macrophage inhibitory cytokine 1 reduces cell adhesion and induces apoptosis in prostate cancer cells. *Cancer Res* 2003; **63**: 5034–5040.
31 Lee DH, Yang Y, Lee SJ, Kim KY, Koo TH, Shin SM *et al.* Macrophage inhibitory cytokine-1 induces the invasiveness of gastric cancer cells by up-regulating the urokinase-type plasminogen activator system. *Cancer Res* 2003; **63**: 4648–4655.
32 Brown DA, Ward RL, Buckhaults P, Liu T, Romans KE, Hawkins NJ *et al.* MIC-1 serum level and genotype: associations with progress and prognosis of colorectal carcinoma. *Clin Cancer Res* 2003; **9**: 2642–2650.
33 Welsh JB, Sapinoso LM, Kern SG, Brown DA, Liu T, Bauskin AR *et al.* Large-scale delineation of secreted protein biomarkers overexpressed in cancer tissue and serum. *Proc Natl Acad Sci USA* 2003; **100**: 3410–3415.
34 Thomas R, True LD, Lange PH, Vessella RL. Placental bone morphogenetic protein (PLAB) gene expression in normal, pre-malignant and malignant human prostate: relation to tumor development and progression. *Int J Cancer* 2001; **93**: 47–52.
35 Yang H, Choi HJ, Park SH, Kim JS, Moon Y. Macrophage inhibitory cytokine-1 (MIC-1) and subsequent urokinase-type plasminogen activator mediate cell death responses by ribotoxic anisomycin in HCT-116 colon cancer cells. *Biochem Pharmacol* 2009; **78**: 1205–1213.
36 Vermeulen SJ, Nollet F, Teugels E, Philippe J, Speleman F, van Roy FM *et al.* Mutation of alpha-catenin results in invasiveness of human HCT-8 colon cancer cells. *Ann NY Acad Sci* 1997; **833**: 186–189.
37 Vermeulen SJ, Debruyne PR, Marra G, Speleman FP, Boukamp P, Jiricny J *et al.* hMSH6 deficiency and inactivation of the alphaE-catenin invasion-suppressor gene in HCT-8 colon cancer cells. *Clin Exp Metast* 1999; **17**: 663–668.
38 Lim do Y, Park JH. Induction of p53contributes to apoptosis of HCT-116 human colon cancer cells induced by the dietary compound fisetin. *Am J Physiol Gastrointest Liver Physiol* 2009; **296**: G1060–G1068.
39 Struckhoff AP, Rana MK, Worthylake RA. RhoA can lead the way in tumor cell invasion and metastasis. *Front Biosci* 2011; **16**: 1915–1926.

40 Rathinam R, Berrier A, Alahari SK. Role of Rho GTPases and their regulators in cancer progression. *Front Biosci* 2011; **17**: 2561–2571.
41 Aepfelbacher M, Zumbihl R, Heesemann J. Modulation of Rho GTPases and the actin cytoskeleton by YopT of Yersinia. *Curr Top Microbiol Immunol* 2005; **291**: 167–175.
42 Chan CH, Lee SW, Li CF, Wang J, Yang WL, Wu CY *et al.* Deciphering the transcriptional complex critical for RhoA gene expression and cancer metastasis. *Nat Cell Biol* 2010; **12**: 457–467.
43 Rihet S, Vielh P, Camonis J, Goud B, Chevillard S, de Gunzburg J. Mutation status of genes encoding RhoA, Rac1, and Cdc42 GTPases in a panel of invasive human colorectal and breast tumors. *J Cancer Res Clin Oncol* 2001; **127**: 733–738.
44 Moscow JA, He R, Gnarra JR, Knutsen T, Weng Y, Zhao WP *et al.* Examination of human tumors for rhoA mutations. *Oncogene* 1994; **9**: 189–194.
45 Faried A, Faried LS, Usman N, Kato H, Kuwano H. Clinical and prognostic significance of RhoA and RhoC gene expression in esophageal squamous cell carcinoma. *Ann Surg Oncol* 2007; **14**: 3593–3601.
46 Dittert DD, Kielisch C, Alldinger I, Zietz C, Meyer W, Dobrowolski F *et al.* Prognostic significance of immunohistochemical RhoA expression on survival in pancreatic ductal adenocarcinoma: a high-throughput analysis. *Hum Pathol* 2008; **39**: 1002–1010.
47 Bellizzi A, Mangia A, Chiriatti A, Petroni S, Quaranta M, Schittulli F *et al.* RhoA protein expression in primary breast cancers and matched lymphocytes is associated with progression of the disease. *Int J Mol Med* 2008; **22**: 25–31.
48 Tong S, Marjono B, Brown DA, Mulvey S, Breit SN, Manuelpillai U *et al.* Serum concentrations of macrophage inhibitory cytokine 1 (MIC 1) as a predictor of miscarriage. *Lancet* 2004; **363**: 129–130.
49 Brown DA, Breit SN, Buring J, Fairlie WD, Bauskin AR, Liu T *et al.* Concentration in plasma of macrophage inhibitory cytokine-1 and risk of cardiovascular events in women: a nested case–control study. *Lancet* 2002; **359**: 2159–2163.
50 Wollmann W, Goodman ML, Bhat-Nakshatri P, Kishimoto H, Goulet Jr RJ, Mehrotra S *et al.* The macrophage inhibitory cytokine integrates AKT/PKB and MAP kinase signaling pathways in breast cancer cells. *Carcinogenesis* 2005; **26**: 900–907.
51 Iczkowski KA, Pantazis CG. Overexpression of NSAID-activated gene product in prostate cancer. *Int J Surg Pathol* 2003; **11**: 159–166.
52 Lu PD, Jousse C, Marciniak SJ, Zhang Y, Novoa I, Scheuner D *et al.* Cytoprotection by pre-emptive conditional phosphorylation of translation initiation factor 2. *EMBO J* 2004; **23**: 169–179.
53 Harding HP, Zhang Y, Zeng H, Novoa I, Lu PD, Calfon M *et al.* An integrated stress response regulates amino acid metabolism and resistance to oxidative stress. *Mol Cell* 2003; **11**: 619–633.
54 Nougayrede JP, Foster GH, Donnenberg MS. Enteropathogenic *Escherichia coli* effector EspF interacts with host protein Abcf2. *Cell Microbiol* 2007; **9**: 680–693.
55 Nagai T, Abe A, Sasakawa C. Targeting of enteropathogenic *Escherichia coli* EspF to host mitochondria is essential for bacterial pathogenesis: critical role of the 16th leucine residue in EspF. *J Biol Chem* 2005; **280**: 2998–3011.
56 Braga V. Epithelial cell shape: cadherins and small GTPases. *Exp Cell Res* 2000; **261**: 83–90.
57 Mahida YR, Rolfe VE. Host–bacterial interactions in inflammatory bowel disease. *Clin Sci (Lond)* 2004; **107**: 331–341.
58 Gradel KO, Nielsen HL, Schonheyder HC, Ejlertsen T, Kristensen B, Nielsen H. Increased short and long term risk of inflammatory bowel disease after Salmonella or *Campylobacter gastroenteritis*. *Gastroenterology* 2009; **137**: 495–501.
59 Mylonaki M, Rayment NB, Rampton DS, Hudspith BN, Brostoff J. Molecular characterization of rectal mucosa-associated bacterial flora in inflammatory bowel disease. *Inflamm Bowel Dis* 2005; **11**: 481–487.
60 Detrich RE. Report on a government sponsored pediatric dental program. *J Maine Med Assoc* 1976; **67**: 52–54.
61 Gotoh T, Oyadomari S, Mori K, Mori M. Nitric oxide-induced apoptosis in RAW 264.7 macrophages is mediated by endoplasmic reticulum stress pathway involving ATF6 and CHOP. *J Biol Chem* 2002; **277**: 12343–12350.

Supplementary Information accompanies the paper on the Oncogene website (http://www.nature.com/onc)